

CHROM. 18 979

COMPARATIVE COMPUTERISED GAS CHROMATOGRAPHIC–MASS SPECTROMETRIC ANALYSIS OF PETROPORPHYRINS

J. P. GILL*, R. P. EVERSLED** and G. EGLINTON*

Organic Geochemistry Unit, School of Chemistry, University of Bristol, Cantock's Close, Bristol BS8 1TS (U.K.)

(Received July 29th, 1986)

SUMMARY

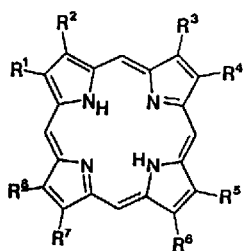
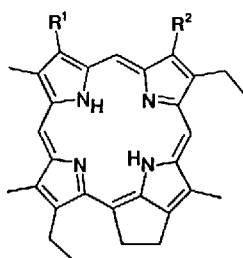
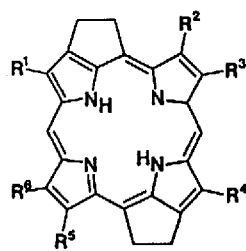
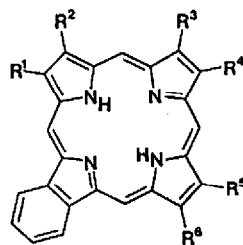
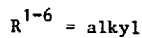
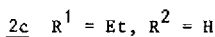
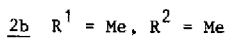
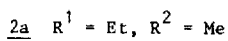
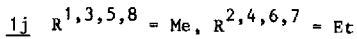
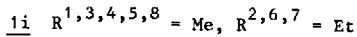
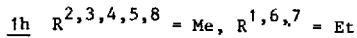
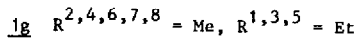
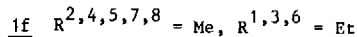
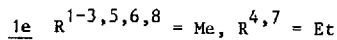
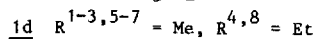
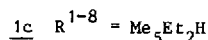
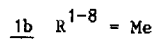
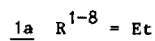
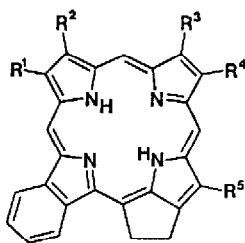
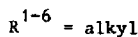
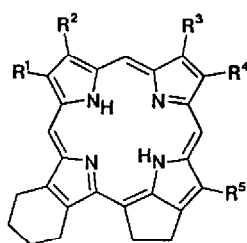
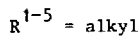
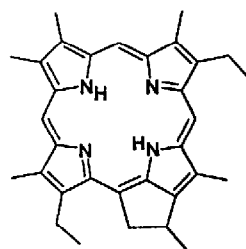
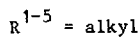
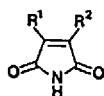
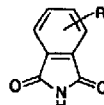
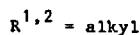
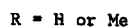
The ability of computerised gas chromatography–mass spectrometry (C–GC–MS) to afford detailed information on petroporphyrin composition is exemplified through analyses of Boscan crude oil and La Luna shale (Maracaibo Basin, W. Venezuela), an oil-source rock pair. The petroporphyrins of both samples are complex mixtures, comprising at least 224 and 175 compounds, respectively. Five structural classes (A, A-2, A-4, A-6 and A-8) have been characterised and shown to contain at least 5 pseudo-homologous series through linear Kováts' plots and co-injection. The two samples are shown to be qualitatively and quantitatively very similar in composition. These related samples are compared and contrasted to an unrelated bitumen, Gilsonite, examined in an earlier paper. The data show that petroporphyrin analysis by C–GC–MS can provide classical biological marker information, *e.g.* thermal maturity. This paper provides the first such comparative examination of petroporphyrins by GC–MS analysis.

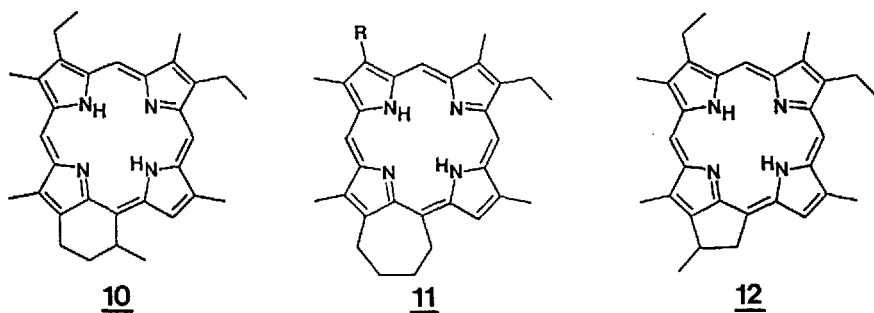
INTRODUCTION

The potential of endogenous petroporphyrins to yield geochemical information such as depositional palaeoenvironment and thermal history is now well established^{1–4}. To obtain such information, the petroporphyrin components must be isolated and characterised. Direct insertion probe mass spectrometry (MS)^{5,6} and high-performance liquid chromatography (HPLC)^{3,7,8} have both been used extensively as means of petroporphyrin “fingerprinting” and characterisation; both have their shortcomings^{9,10}. We have recently developed procedures whereby petroporphyrins can be rigorously analysed by computerised gas chromatography–mass spectrometry (C–GC–MS) as their bis(*tert.*-butyldimethylsiloxy)Si(IV) derivatives. Porphyrin com-

* Present address: Shell Research Ltd., Sittingbourne Research Centre, Sittingbourne, Kent ME9 8AG, U.K.

** Present address: Department of Biochemistry, University of Liverpool, P.O. Box 147, Liverpool L69 3BX, U.K.

123456978



11a R = Me

11b R = Et

position is readily determined⁹⁻¹³. Structural type is deduced from the characteristic $(M - 131)^+$ ions. Further classification into pseudo-homologous series is achieved via assignment of pseudo-Kováts retention indices and co-chromatography of derivatised standards of known structure. Quantitative information, readily obtainable from ion-intensity data, can be used to plot distribution profiles for use in comparative studies.

The procedural details of the C-GC-MS and data handling techniques are well documented^{10,13,14}. To date, however, detailed analysis has been reported for only a single sample, the Gilsonite bitumen (Eocene, Uinta Basin, UT, U.S.A.)¹⁴. The results demonstrated the power of the technique to yield compositional information inaccessible by other methods. Over 100 individual components were observed, comprising four structural classes.

We now extend C-GC-MS investigations of petroporphyrins to Boscan crude oil and its proposed source rock, the La Luna shale (Cretaceous, Maracaibo Basin, W. Venezuela). Studies of the Maracaibo Basin have firmly demonstrated this source-oil relationship^{15,16}. Petroporphyrin analysis has been used to establish this close relationship¹⁷. The oils and shales of this region are well known for their high vanadyl porphyrin content (typically several thousand ppm of the crude oils and shale extracts) and have been the subject of a number of porphyrin investigations. Ultraviolet-visible spectrophotometry (UV-VIS) initially revealed their high vanadyl porphyrin content¹⁷. Subsequently^{5,6}, MS of both metallo- and metal-free (following sequestration in acid media) porphyrins showed them to be a complex mixture of structural types proposed to be aetio (1), deoxophylloerythroaetio-(DPEP; 2), di-DPEP (3), rhodo-aetio- (4) and rhodo-DPEP (5). Recently, the nomenclature benz-aetio- and benz-DPEP- has been used for the latter two structural types² on the basis of structures (4 and 5) suggested earlier⁶. Structures of the benz-DPEP type have now been proven unambiguously for two compounds (C_{32} and C_{33})¹⁸. ¹H NMR evidence has been presented⁴ for the structure of the so-called di-DPEP porphyrins; a tetrahydro-benz-DPEP structure (6) was proposed. Extensive carbon number homology has been detected by MS for the various proposed structural types^{5,6,19-21}. Chromium trioxide oxidation of Boscan porphyrins has been employed in attempts to determine the nature of β -alkyl substituents of the porphyrin ring^{20,22-24}. GC-MS

analyses showed the presence of maleimide (7) and phthalimide (8) oxidation products. Hence, evidence was obtained for the presence of compounds bearing extended β -alkyl substituents²⁴ and fused benzo-rings²⁰; both structural features are unknown in modern-day biogenic porphyrins. The presence of fused benz(o) rings in some compounds has recently been unambiguously proved¹⁸. Thin-layer chromatography (TLC) and HPLC of Boscan porphyrins have been used to afford carbon number separations^{7,25}. Kováts'-type plots of log isocratic retention times vs. carbon number provided evidence for the presence of at least three homologous or pseudohomologous series of aetioporphyryns in Boscan oil and La Luna shale²⁶. Indications of pseudo-homologous series were also obtained in early GC-MS examinations of Boscan porphyrins on packed GC columns²⁵. The poor resolution and high adsorptive properties of the packed GC columns limited further investigation²⁷ and led us to employ flexible fused silica capillaries and bonded phases in order to obtain the detailed C-GC-MS information required^{9,11,12,28}.

It was envisaged that analyses of the Boscan and La Luna petroporphyrins would enable us to begin to test the versatility of the C-GC-MS data for use in comparative geochemical investigations. Furthermore, by choosing samples that have experienced very different geological histories to the Gilsonite bitumen (the only other sample so far studied and reported in this way¹⁴) it may be possible to build up an explicit picture of the way in which petroporphyrin content and distributions vary with differing geological regimes.

EXPERIMENTAL

Samples

The geological histories of the La Luna shales and Boscan oils have been described in detail elsewhere^{17,29}. The oil examined was Boscan 8E-4, which had been studied previously by TLC, HPLC and MS^{8,17}. The La Luna sample examined herein was obtained from an outcrop in the type-area. Gilsonite data derive from an earlier publication¹⁴.

Extraction of free-base porphyrins

After Soxhlet extraction of the shale (83 h, dichloromethane), the porphyrins were extracted as their free bases by demetallation with methanesulphonic acid, according to established procedures³⁰. Typically, crude oil or shale extract (1 g) was heated (100°C, 2 h) with at least a five-ten fold excess of methanesulphonic acid (98%, ca. 10 ml, Aldrich). The reaction was quenched by pouring the acid-organic mixture into distilled water (25 ml). After allowing to cool, the coagulated organic material was removed by filtration. The aqueous filtrate, containing the porphyrins as dications, was extracted with dichloromethane (3 × 15 ml), which was then neutralised (sodium bicarbonate) and dried (sodium sulphate). The free-bases obtained were purified by TLC (silica gel-dichloromethane). In neither the Boscan nor La Luna case was separation of nickel and vanadyl porphyrins attempted. In each case the nickel porphyrins are present in much lower abundance (< 100 ppm)³¹.

La Luna shale (513 g) produced a total extract (7.7 g) yielding free-base porphyrins (127 mg: 247 ppm of shale, 1500 ppm of extract). Boscan oil (1 g) yielded free-base porphyrins (2.5 mg: 2500 ppm of oil). All UV-VIS spectra were recorded

in dichloromethane solution, quantification being performed on the α absorption maximum of the vanadyl porphyrins (570 nm, $\epsilon = 17\ 600$)³² or absorption band IV of the free-base porphyrins (498 nm, $\epsilon = 15\ 600$)³².

Compounds for co-injection

The compounds employed in the co-injection studies were those used earlier¹⁴. The compound identities, their structure references, pseudo-Kováts retention indices [KRI, as (TBDMSO)₂Si derivatives], MS ($M - 131$)⁺ ion m/z , source, and occurrence in La Luna shale and Boscan crude oil are listed in Table I.

Friedel-Crafts acetylation

An aliquot of the free-base porphyrins from Boscan oil was converted to its copper(II) chelates³⁹ prior to acetylation⁴⁰, as described previously for Gilsonite¹⁴. TLC separation yielded a fully β -alkyl substituted fraction which was derivatised for GC-MS analysis.

Derivatisation

The insertion of silicon into aliquots of the free-bases and formation of (TBDMSO)₂Si derivatives was carried out as described earlier^{9,14}.

Instrumentation, data acquisition and KRI calculation

The instrumentation and data acquisition parameters have been fully detailed elsewhere¹⁴. GC-MS analyses were performed on a Finnigan 4000 quadrupole mass spectrometer, linked to a Finnigan 9610 gas chromatograph with modified SGE OCI-2 on-column injector. The column was a flexible fused-silica capillary (Hewlett Packard "Ultra" series; 25 m \times 0.31 mm I.D.) coated with cross-bonded polydimethylsiloxane (0.17 μ m film thickness); temperature programming details as for the Gilsonite analyses¹⁴. Data acquisition was in multiple ion detection (MID) mode monitoring the ion m/z 113 and then scanning the range m/z 545–850¹⁴. Data processing utilised a Finnigan INCOS 2300 data system.

Retention indices were calculated by computer program (RRI⁴¹), using *n*-alkane standards⁴². Improved reproducibility of KRI calculation was achieved by use of two standard porphyrin derivatives [(TBDMSO)₂Si OMP and (TBDMSO)₂Si OEP (Table I)] as retention standards, their pseudo-Kováts retention indices being defined as 3455 and 3800, respectively. The KRI values of the more numerous *n*-alkanes were then adjusted in the RRI program by a constant offset (generally < 10 KRI units) until these defined values were realised. Thus, problems caused by differences in GC behaviour of the porphyrin derivatives and the *n*-alkanes are effectively minimised.

Processing of GC-MS data

Detailed data processing for the Boscan and La Luna samples followed the procedures described previously^{9,13,14}.

Data presentation

The presentation of data in this paper, while developed from our earlier published methods^{9,14}, has been designed to allow direct comparison of multiple sample analyses in a variety of ways.

Figs. 1 and 2 show simple GC-MS reconstructed ion current (RIC) traces presented on a KRI scale vs. ion intensity. The regions above KRI 3775 have been expanded by a factor of 5 in the vertical scale.

Figs. 3 and 4 contain plots of KRI vs. carbon number. Rather than showing all the points (\equiv porphyrins detected) for one sample (*cf.* Figs. 3-6, 8 of ref. 14), the

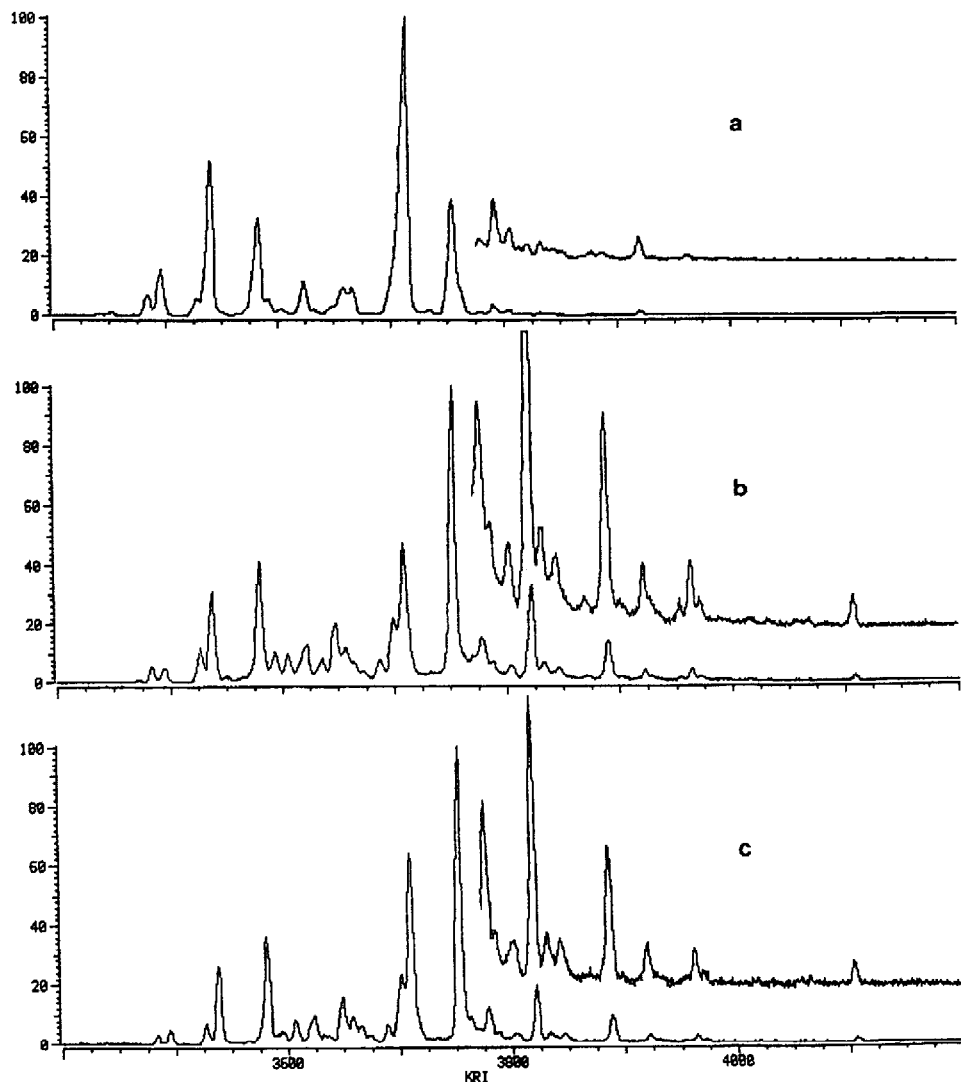


Fig. 1. Reconstructed ion current (RIC; m/z 545-850) GC-MS traces for the total porphyrin mixtures [as their $(\text{TBDMSO})_2\text{Si}$ derivatives] of (a) Gilsonite bitumen, (b) La Luna shale, and (c) Boscan oil. The retention time scale has been converted to KRI by computer interpolation, using data for co-chromatographed *n*-alkanes. Considerable co-elution of components is occurring but some peaks are broad and fronting due to high loading of the GC column, required to enable detection of trace components. Injection of *ca.* 1-5 μg of porphyrin derivatives on-column produced ion intensity values for the largest peak of 206 592 (a), 56 896 (b) and 45 312 (c). See Experimental for conditions.

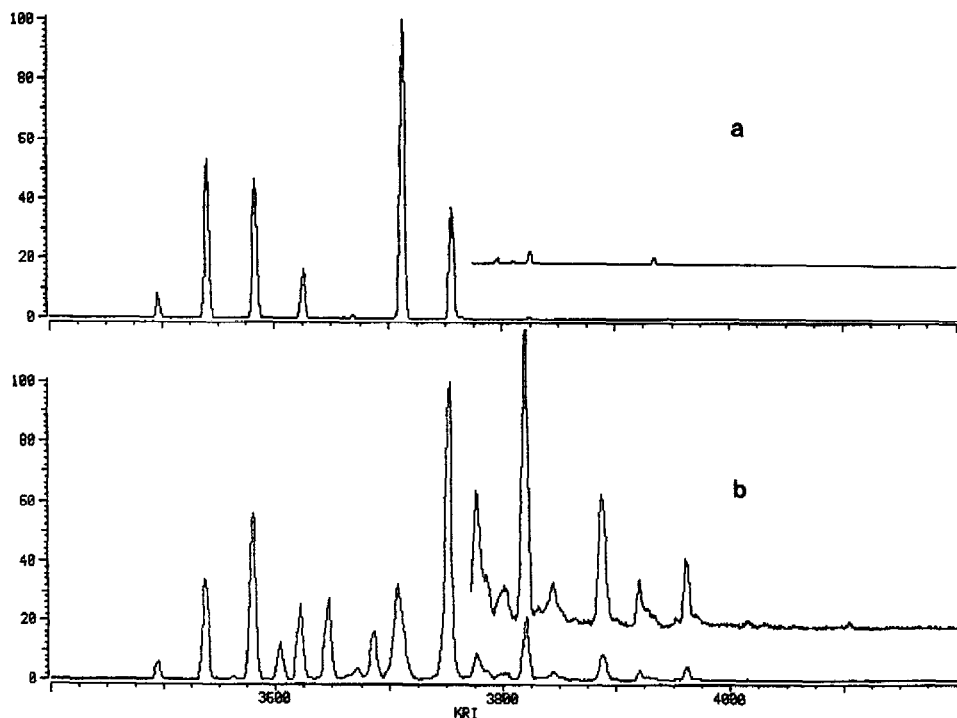


Fig. 2. RIC (m/z 545–850) traces for the fully alkylated petroporphyrin fractions [as their $(\text{TBDMSO})_2\text{Si}$ derivatives] of (a) Gilsonite bitumen and (b) Boscan oil. Compared to Fig. 1, the greatly improved peak shapes are the consequence of simplification brought about by the removal of β -unsubstituted components, so eliminating much of the co-elution found in the total mixtures. Column loadings are comparable, with ion intensities of 281 088 (a) and 78 208 (b). See Experimental for details.

plots show comparisons of two samples. Thus, Fig. 3a contrasts the porphyrin content of La Luna shale with the unrelated Gilsonite bitumen; Fig. 3b compares the shale with its sourced oil, Boscan; and Fig. 4 contrasts only the fully alkylated porphyrins of Gilsonite and Boscan. In each plot, a carbon number range of 27–36 has been used. Some samples (especially Boscan, Table II) contain porphyrins outside this range, but these fall below the abundance thresholds used. Only porphyrins having abundances $>2\%$ of the largest have been displayed in the A and A-2 class plots, and only those $>0.4\%$ of the largest in the A-4, A-6 and A-8 classes. Each plot has a vertical axis range of 500 KRI units, the actual range chosen is varied to suit the class (e.g. 3400–3900 for the A class, 3800–4300 for the A-8 class).

Fig. 5 contains histograms of abundance (\equiv ion intensity) vs. carbon number for the five petroporphyrin series partially identified (by co-chromatography and KRI comparisons) in the three samples studied. The use of carbon number rather than KRI as the horizontal scale allows more direct comparison of samples (*cf.* Fig. 7 of ref. 14). Abundances are normalised to the largest individual component as 100%.

Fig. 6 contains similar histograms to the above, but for the five unsaturation classes found in these samples. The abundances are normalised to the largest total

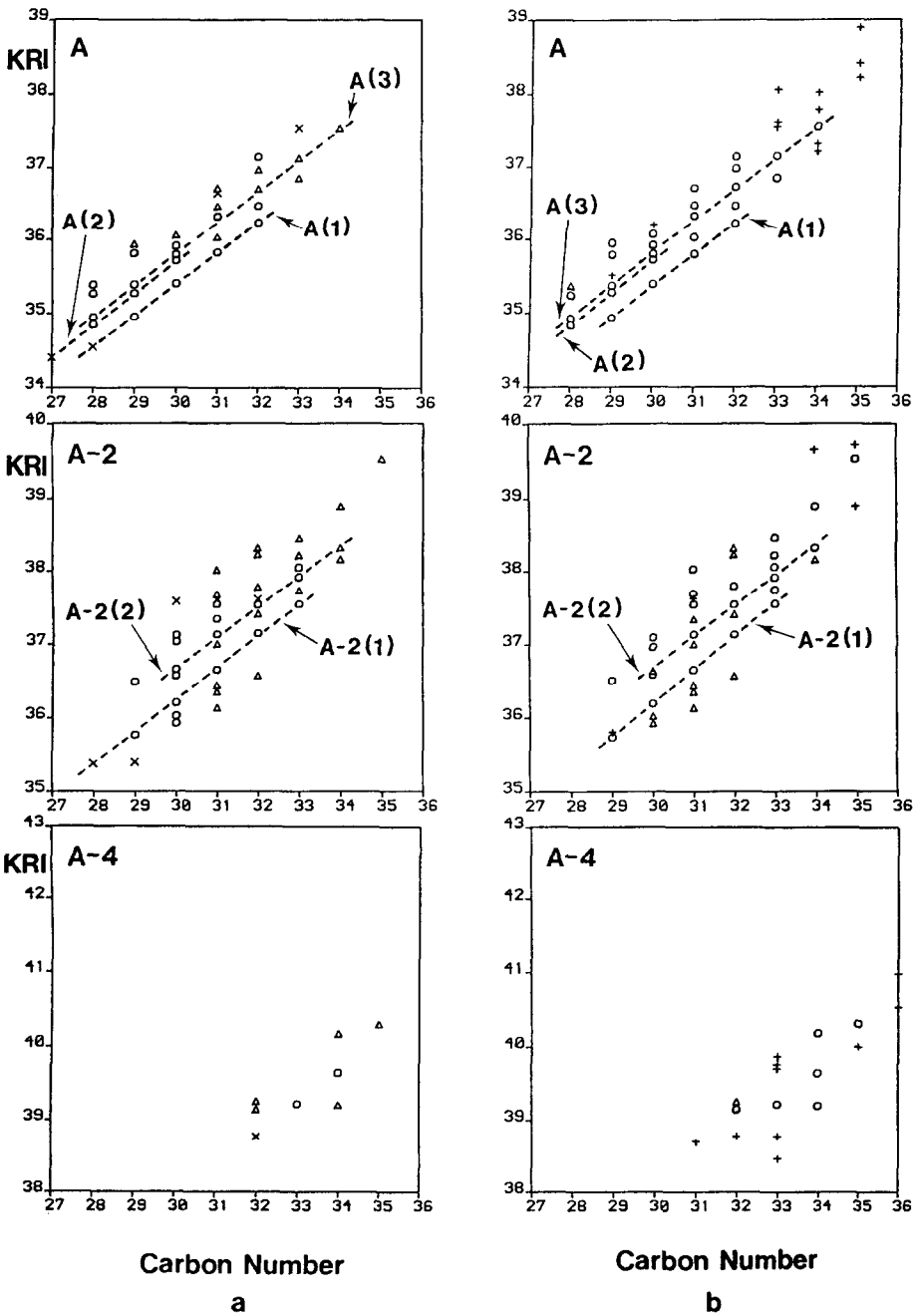


Fig. 3.

(Continued on p. 290)

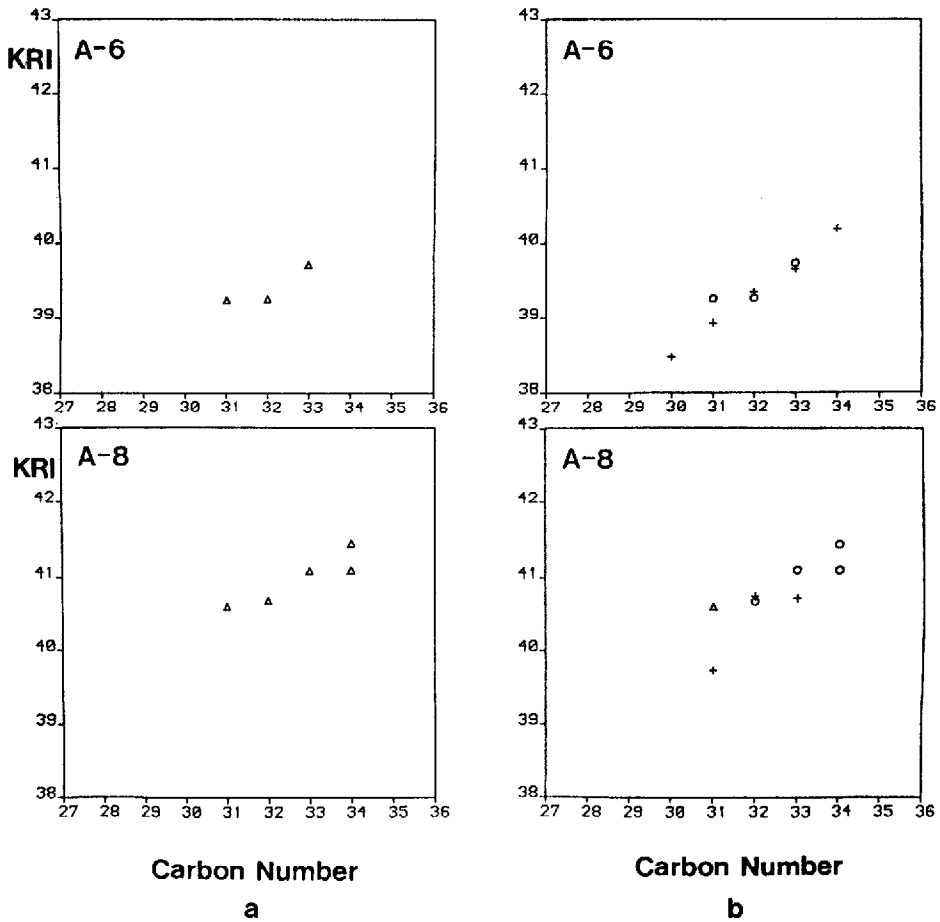


Fig. 3. Plots of KRI vs. carbon number for GC-MS analyses of porphyrins as their (TBDMSO)₂Si derivatives, comparing the petroporphyrin compositions, displayed as A, A-2, A-4, A-6 and A-8 classes for (a) La Luna shale and the unrelated Gilsonite bitumen, (b) La Luna shale and its sourced oil, Boscan. Before being plotted, threshold values of intensity were applied to reduce the number of points. The lower limits used were > 2% of the largest peak for A and A-2 classes, and > 0.4% of the largest peak for A-4, A-6 and A-8 classes. Different symbols illustrate those points (\equiv porphyrin components) common to two samples, present only in one sample, or only in the other sample (see key). Dashed lines indicate proposed pseudo-homologous series^{1,4}, partially identified by co-chromatography or KRI and MS comparison. Experimental conditions were as for Figs. 1 and 2 (see text). Key: (a) x, Gilsonite only; Δ, La Luna only; ○, Gilsonite and La Luna; (b) Δ, La Luna only; +, Boscan only; ○, La Luna and Boscan.

carbon number as 100% and these plots include all porphyrins detected in the C₂₆-C₃₈ range.

Fig. 7 contains histograms for all the pseudo-homologous series co-injected or KRI compared with the samples, even where the series represented by the standards was not present in the samples. All are normalised to the largest individual compound as 100%. Histograms are included for the sum of those compounds remaining after the partially identified series have been subtracted from the total for that class. This

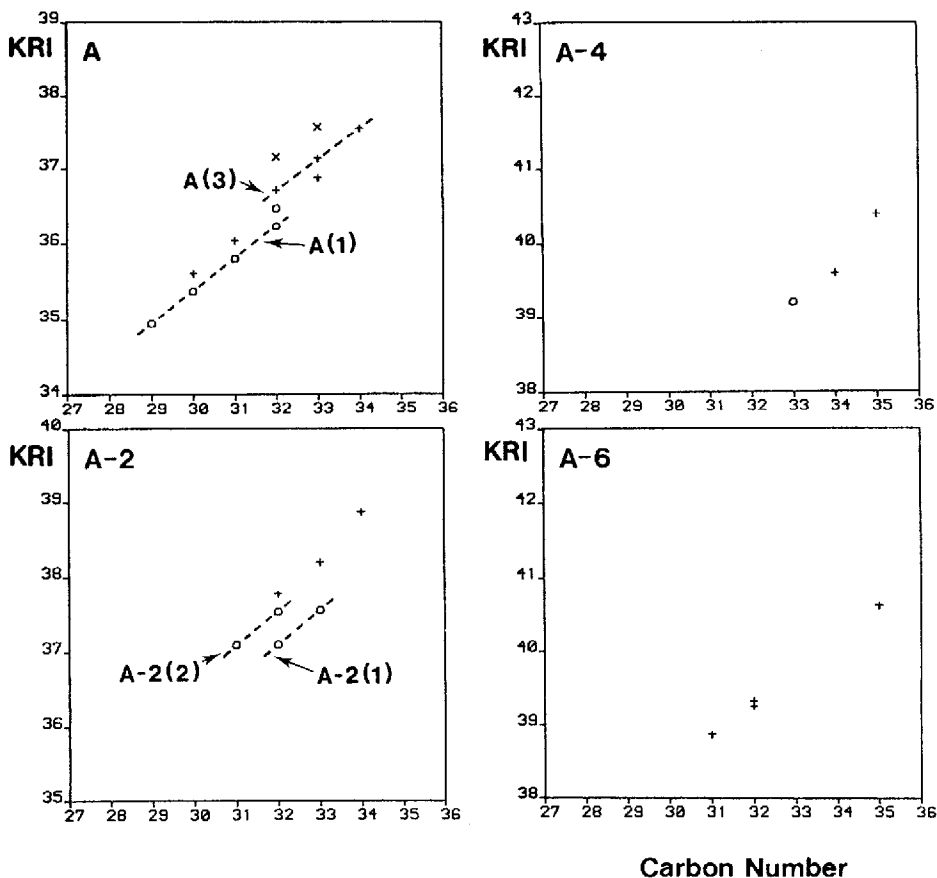


Fig. 4. Plots of KRI vs. carbon number comparing the A, A-2, A-4 and A-6 classes of porphyrins in the fully alkylated fractions of Gilsonite bitumen and Boscan oil, as their $(\text{TBDMSO})_2\text{Si}$ derivatives. The simplification which has ensued following removal of β -unsubstituted porphyrins is evident by comparison with Fig. 3. However, such removal may not be complete (see text). Thresholds are applied as for Fig. 3; A-8 class porphyrins were below 0.4% of the largest peak. Again, different symbols are used to show common components and those present only in one or other of the samples (see key). Pseudo-homologous series are indicated by dashed lines. Experimental conditions were as for Figs. 1 and 2 (see text). Key: \times , Gilsonite only; $+$, Boscan only; \circ , Gilsonite and Boscan.

figure forms the basis for expansion as further series are identified and co-injected (e.g. structures $2c^{43}$, 12^{44}). In Figs. 3-7, components were assumed to be identical in two samples if possessing identical mass spectral ions and KRI values within ± 5 units.

Tables III and IV are similar to Table III of ref. 14. It should be noted that components are listed below each carbon number in order of elution, so that horizontal rows do not represent pseudo-homologous series.

TABLE II

CARBON NUMBER RANGES AND MAXIMA OF THE FIVE UNSATURATION CLASSES OF PORPHYRINS OBSERVED IN GILSONITE BITUMEN, LA LUNA SHALE AND BOSCAN OIL, AS DETERMINED BY C-GC-MS

n.d. = Not detected.

Class	Carbon number range (maximum)		
	<i>Gilsonite</i>	<i>La Luna</i>	<i>Boscan</i>
A	26-35 (30)	26-36 (30)	27-38 (30)
A-2	27-35 (31)	27-36 (32)	28-38 (32)
A-4	31-34 (33)	31-36 (34)	31-37 (34)
A-6	31-34 (32)	31-34 (33)	30-34 (32)
A-8	n.d.	31-34 (33)	31-36 (33)

RESULTS

Gilsonite bitumen

The extraction, demetallation and derivatisation of the petroporphyrins of *Gilsonite* have been described in detail elsewhere¹⁴. Some results are repeated and extended herein, with display formats chosen to allow comparison with *La Luna* shale and *Boscan* oil.

La Luna shale

Fig. 1b shows the RIC (m/z 545-850) obtained from the total petroporphyrin derivatives of *La Luna* shale. Thirty-five fully or partially resolved peaks are discernable. As is generally the case in GC-MS analysis of complicated mixtures, considerable co-elution of components is occurring, as evidenced by subsequent mass chromatography. Single-ion mass chromatograms were examined for the intense $(M-131)^+$ ions of all alkyl porphyrins from C_{20} to C_{42} , and for the classes A, A-2, A-4, A-6 and A-8. The porphyrins present were of the carbon numbers and classes listed in Table II. To enable the checking of mass chromatogram peaks, spectra were obtained, summed in groups of 20 scans, sequentially over the entire region of porphyrin elution. These were processed to allow the detection and rejection of "spurious" peaks, *i.e.* peaks not due to $(M-131)^+$ ions of porphyrin derivatives (discussed in detail elsewhere⁹). The remaining "genuine" mass chromatogram peaks were listed (Table III). Quantification of the detected porphyrin derivatives listed in Table III was performed by published methods¹⁴, and is therefore subject to the same errors arising when two porphyrins, with masses differing by two a.m.u., co-elute (*e.g.* a C_{30} A class porphyrin co-elutes with a C_{30} A-2 class porphyrin at KRI 3620 (see Table III). Such instances of co-elution occurred 28 times in the *La Luna* analysis, the quantification error introduced from this source varying from being negligible (<1%, where the compound of lower mass is much less abundant than that of higher mass) to a worst case in which a compound, though present, is not detected, because its $(M-131)^+$ ion is "swamped" by the isotope peak of a co-eluting

compound. The approximate quantification adopted was, therefore, simply to use the peak areas of the characteristic $(M - 131)^+$ ions in the GC-MS data. These areas were obtained from retention index (RI) lists, output by program RRI⁹. The areas of the peaks may be read directly from the list, and are then expressed as fractions (%) of the area of the major C₃₂ A-2 porphyrin (KRI = 3754, 2a), read from the m/z 633 list, and also as fractions of the total porphyrins. Table III contains details of each porphyrin detected by GC-MS analysis of the petroporphyrins of La Luna shale (175 in all), its class, carbon number, KRI and abundance.

To allow further investigation of the tabulated petroporphyrins, Kováts' plots were prepared. For the porphyrins within each class (A, A-2, etc.), KRI was plotted against carbon number after application of threshold values (see *Data presentation*). Two sets of plots show comparative co-plotting of data from Gilsonite and La Luna (Fig. 3a), and La Luna and Boscan (Fig. 3b). The series partially identified in Gilsonite¹⁴ are present also in La Luna and are marked on the plots by dashed lines.

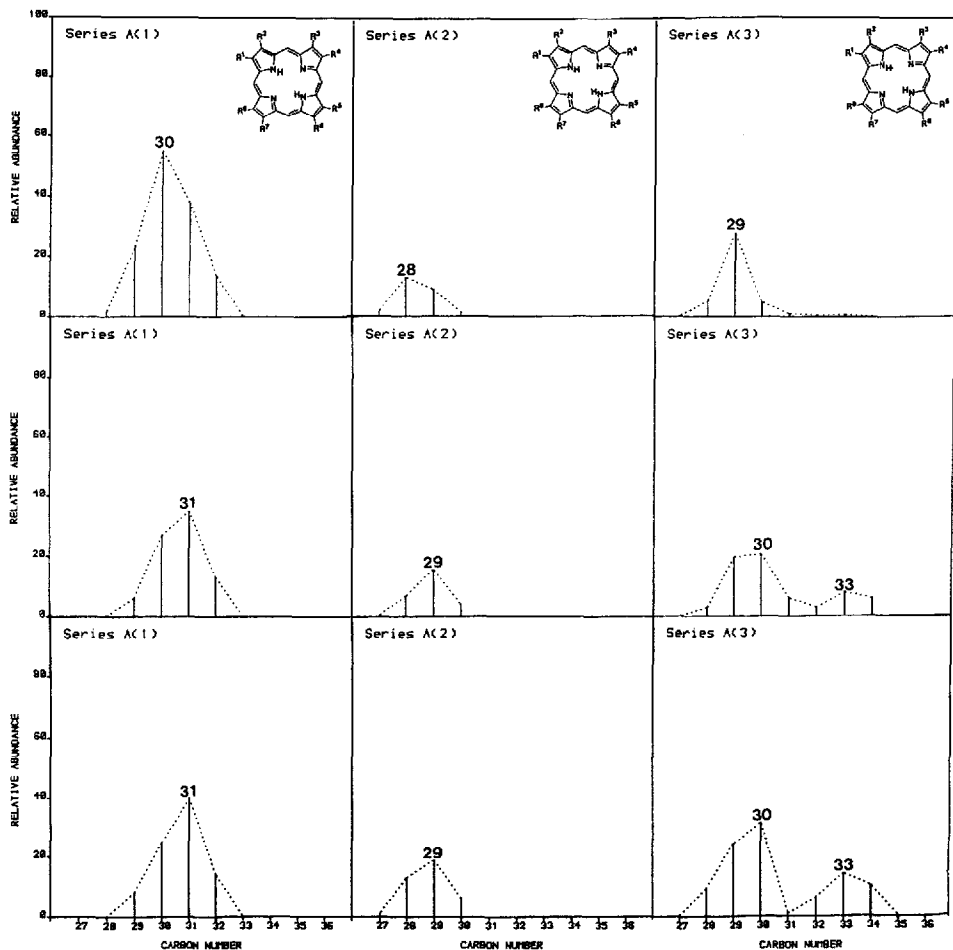


Fig. 5.

(Continued on p. 294)

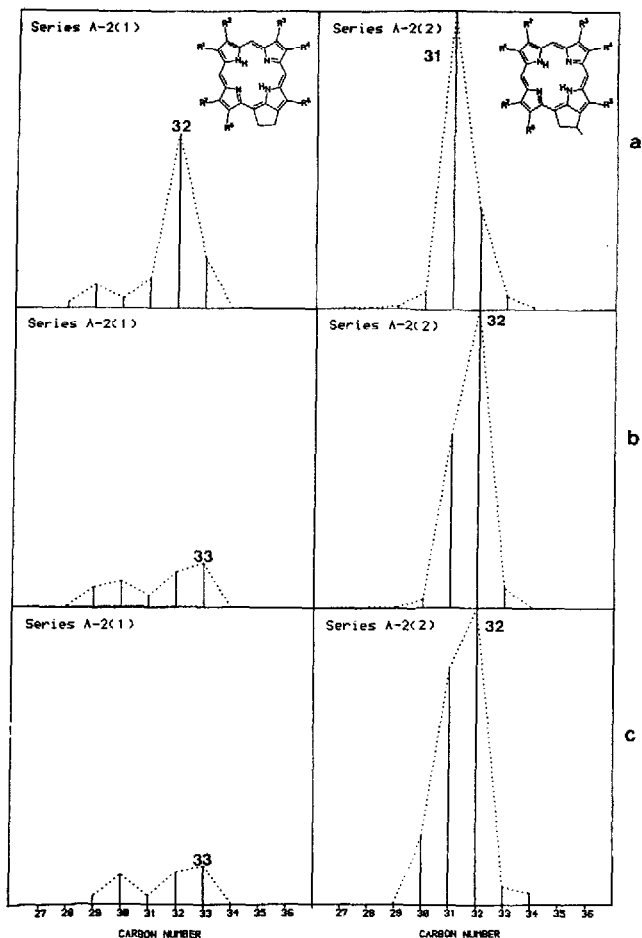


Fig. 5. Relative abundance histograms for the five partially identified series of petroporphyrins occurring in (a) Gilsonite bitumen, (b) La Luna shale, and (c) Boscan oil. Assignment is based on similarity (± 5) of KRI values to those of derivatised porphyrins of known structure and by extrapolation from them on Kováts' plots (see Fig. 3a,b). Abundances are derived from ion intensity data⁹. Compounds of elucidated structure which have been co-injected are: A(1) series, C₃₀, C₃₁ and C₃₂; A(2) series, C₂₉ (partially identified); A(3) series, C₂₉ (partially identified); A-2(1) series, C₃₂; A-2(2) series, C₃₁ and C₃₂. The structure of A(1) C₂₉ is known from comparison of abundance with the work of Quirke *et al.*³³. As contrasted to ref. 14, the data are plotted here by carbon number rather than KRI, allowing more direct comparison between different samples, in which KRI values differ by up to ± 5 units for the same components.

There is reason to suppose, by analogy with the behaviour of standards, that if the points on the Kováts' plots are joined by straight lines with gradients of *ca.* 40–50 KRI units per carbon number, then these lines represent pseudo-homologous series of structurally related petroporphyrins. Further evidence for this hypothesis has come from co-injection experiments. Table I sets out the standards employed, their GC–MS characteristics (KRI values and major MS ions), and indicates occurrences of co-incidence with a component of the La Luna porphyrins. Co-injection

experiments with standard porphyrin derivatives were not performed for La Luna shale. Knowledge of the retention indices of the standards concerned (Table I), and of the coincidence of straight-line relationships of the La Luna Kováts' plots with those of Gilsonite¹⁴ and Boscan, allows reliable identification of those components of the La Luna porphyrin mixture which correspond to the known standards. Thus, for example, it is possible to state that the C₃₀ aetioporphyryn (KRI = 3539; Table III) is identical to, or isomeric with, the C₃₀ aetioporphyryn isolated from Gilsonite (Id or 1e³⁴).

By use of the KRI comparison method, a number of compounds have been tentatively identified in the petroporphyrins of La Luna shale, certain other compounds can be definitely stated to be absent from the mixture (or, at least, to be below the GC-MS detection limit for (TBDMSO)₂Si derivatives). The standard porphyrins are listed in Table I, showing whether or not they are present in La Luna shale.

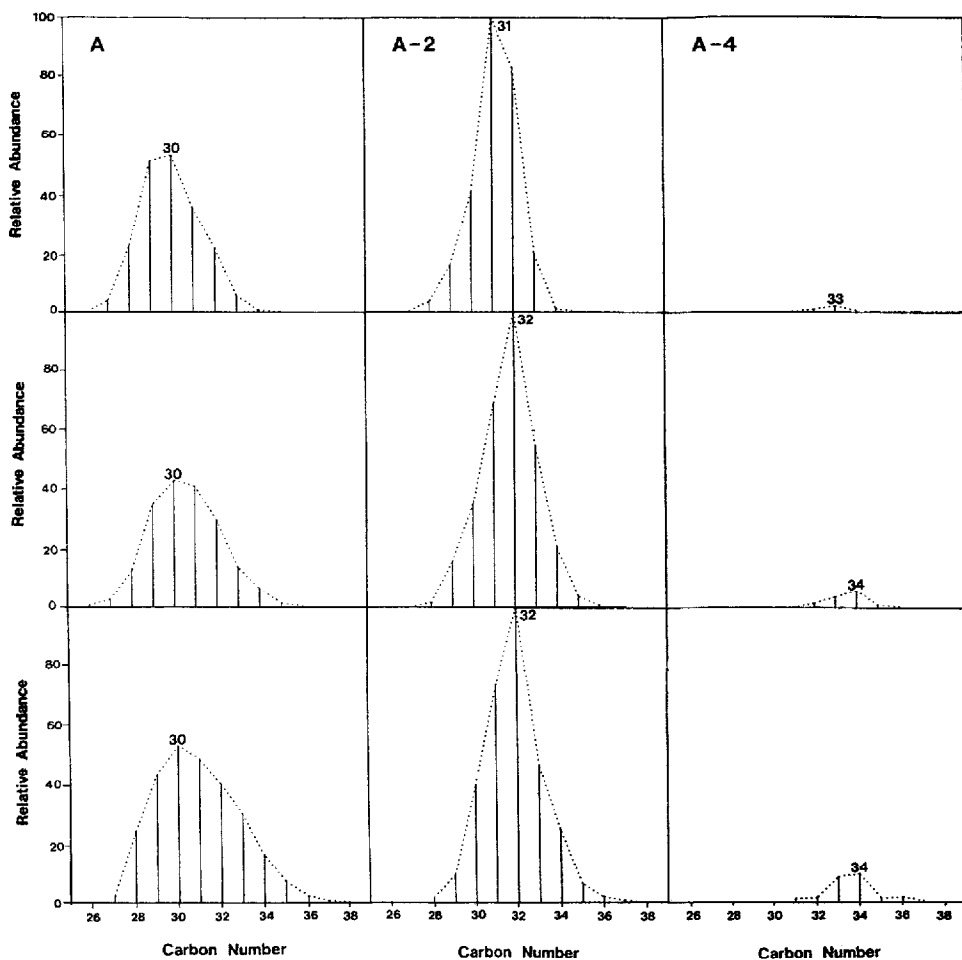


Fig. 6.

(Continued on p. 296)

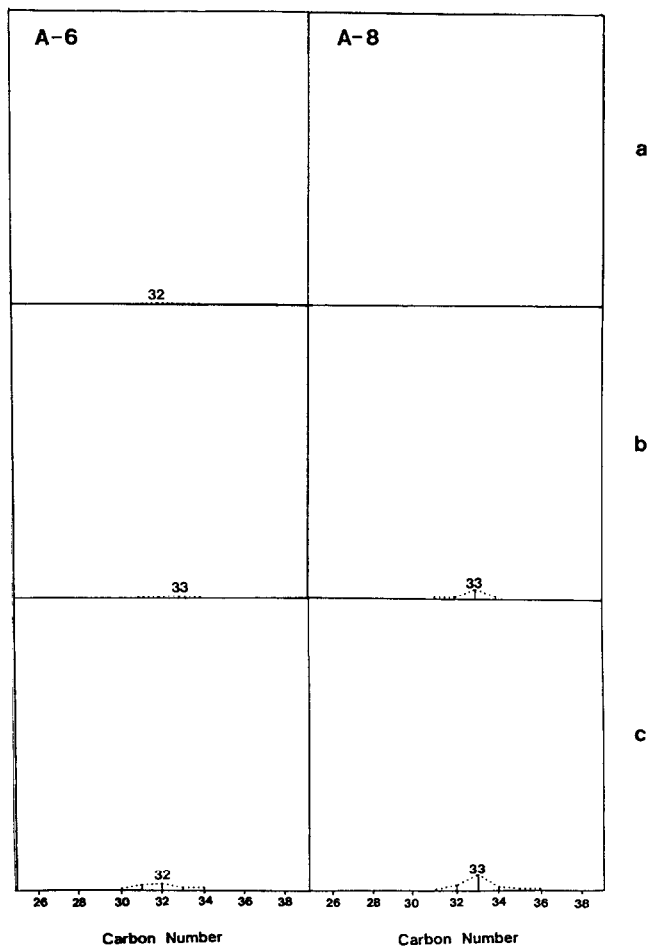


Fig. 6. Relative abundance histograms for the 5 unsaturation classes A, A-2, A-4, A-6, A-8, as detected in (a) Gilsonite, (b) La Luna, and (c) Boscan samples.

Following this procedure, five pseudo-homologous series of petroporphyrins may be partially identified, as for Gilsonite bitumen¹⁴: A(1), A(2), A(3), A-2(1) and A-2(2).

Histograms (Fig. 5b) were prepared for each of the five series, forming distribution profiles, showing each component of the series, with its KRI value and relative abundance. In each case, the abundances are presented as percent fractions of the abundance of the C₃₂ A-2 of KRI = 3754 (structure 2a). Additional histograms of this type are shown in Fig. 6b. These show the abundance and carbon number relationships within the unsaturation classes, A, A-2, A-4, A-6 and A-8. Histograms of different types appear in Fig. 7b, showing all the series for which standards were available, plotting abundance against carbon number for each series A(1), A(2), A(3), A-2(1) and A-2(2). In addition, series A-2(3) and A-2(4) appear. These have structures as shown and are included, though absent from the samples studied in this

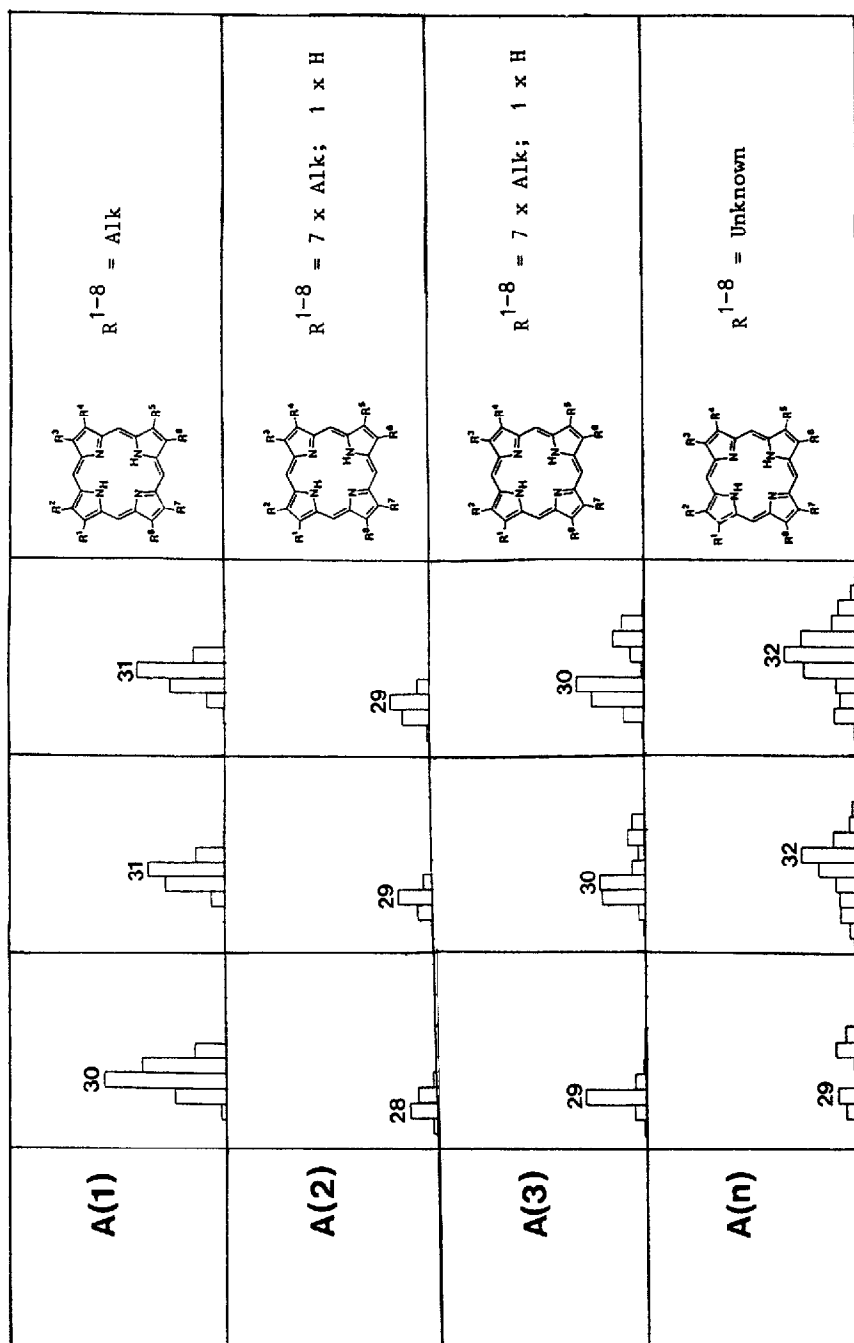
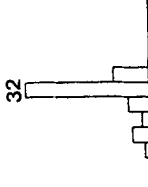

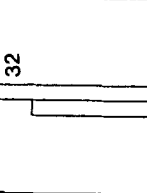
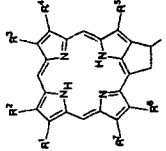
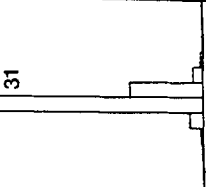
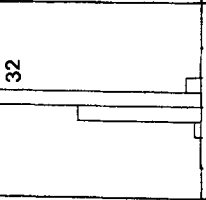
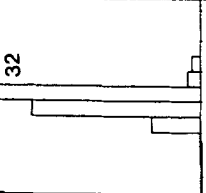
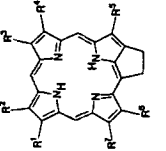
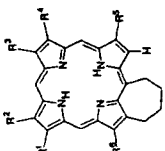
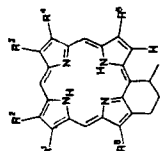


Fig. 7.

(Continued on p. 298)

A-2(1)				<p style="text-align: center;">$R^{1-7} = \text{Alk}$</p> 
A-2(2)				<p style="text-align: center;">$R^{1-7} = \text{Alk}$</p> 
A-2(3)				<p style="text-align: center;">$R^{1-6} = \text{Alk}$</p> 
A-2(4)				<p style="text-align: center;">$R^{1-6} = \text{Alk}$</p> 

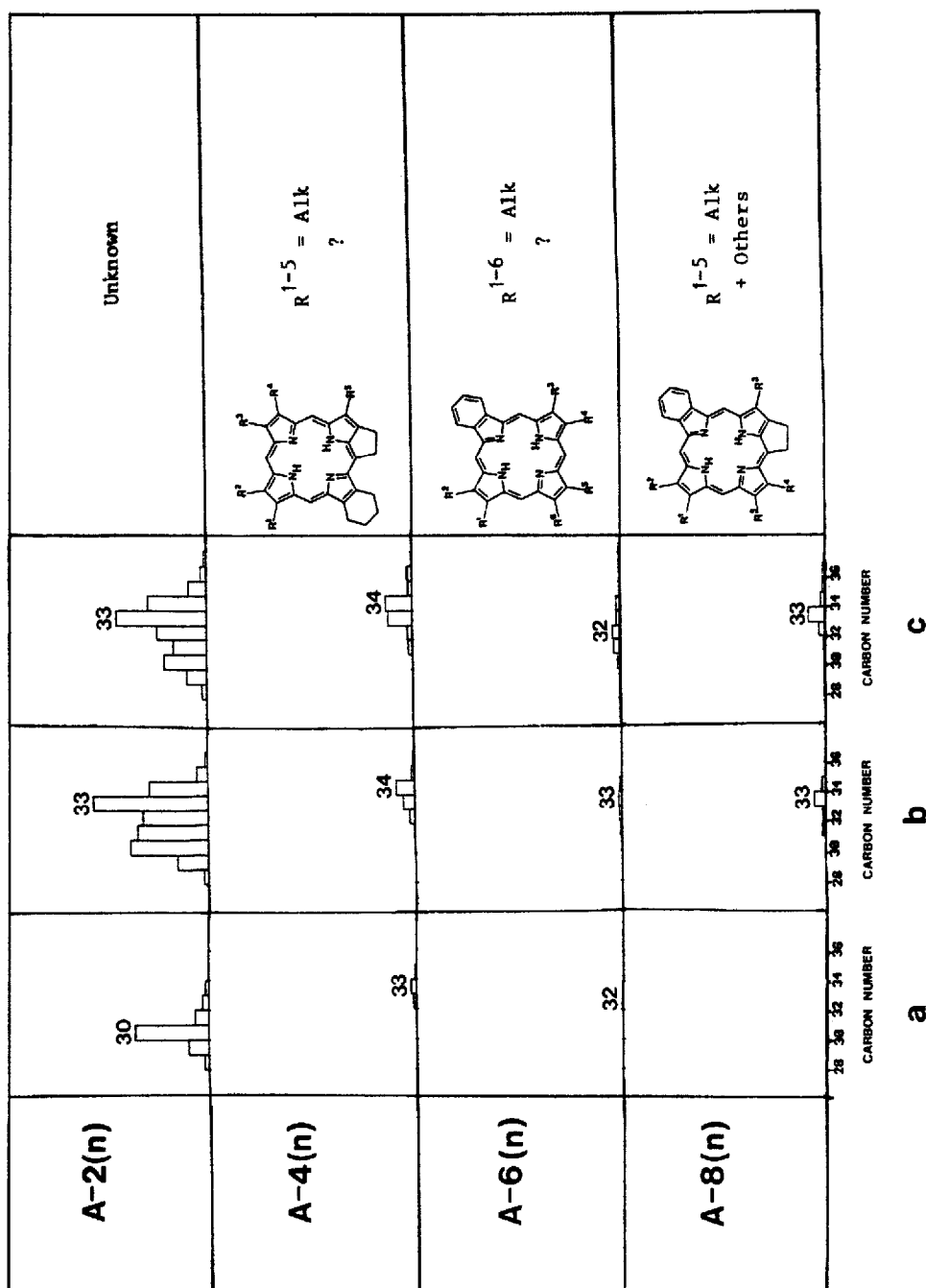


Fig. 7. Relative abundance histograms for the series of porphyrins identified to date in geological materials by C-GC-MS analysis. Results are presented for three samples and 12 series. The samples are labelled across the x-axis and the series in the left hand column, with partial structures to the right of the histograms, where known. Series names are as used previously, with the addition of series A(n), A-2(n), A-4(n), A-6(n) and A-8(n) to include all compounds not assigned to one of the partially identified series. a, Gilsonite; b, La Luna; c, Boscan.

TABLE III
 PETROPORPHYRINS DETECTED BY GC-MS ANALYSIS OF LA LUNA SHALE

tr = less than 0.1% of total petroporphyrins.

Class	Carbon number, retention index (KRI), relative abundance (%) [*]											
	26	27	28	29	30	31	32	33	34	35	36	
A	3426 (0.2:tr)	3441 (0.5:tr)	3455 (0.2:tr)	3495 (6:0.8)	3539 (27:4)	3580 (35:5)	3622 (13:1.8)	3666 (0.1:tr)	3755 (6:0.8)	3820 (0.8:0.1)	3884 (0.1:tr)	
	3437	3448	3483	3527	3572	3604	3647	3687	3778	3823	3928	
	(0.2:tr)	(0.4:tr)	(7:1.0)	(16:2)	(4:0.5)	(8:1.1)	(16:2)	(9:1.2)	(1:0:0.1)	(0.4:tr)	(0.3:tr)	
	3447	3468	3493	3537	3579	3633	3672	3714	3800	3837	3960	
	(0.2:tr)	(1.4:0.2)	(3:0.4)	(20:3)	(21:3)	(6:0.8)	(3:0.4)	(8:1.1)	(1:0:0.1)	(0.1:tr)	(0.1:tr)	
	3467	3482	3523	3551	3592	3648	3698	3751	3816	3859		
	(0.1:tr)	(1.2:0.2)	(5:0.7)	(0.9:0.1)	(5:0.7)	(8:1.1)	(5:0.7)	(0.5:tr)	(0.6:tr)	(0.2:tr)		
	3487	3492	3537	3579	3607	3673	3714	3757	3849	3890		
	(0.3:tr)	(0.3:tr)	(2:0.3)	(4:0.5)	(2:0.3)	(2:0.3)	(5:0.7)	(1.4:0.2)	(0.6:tr)	(0.5:tr)		
	3498		3554	3595	3619		3731	3772				
	(0.3:tr)		(0.8:0.1)	(3:0.4)	(1.5:0.2)		(0.3:tr)					
					3655							
					(1.3:0.2)							
	A-2	3528	3527	3528	3527	3578	3614	3658	3755	3799	3886	3968
		(0.3:tr)	(0.2:tr)	(0.3:tr)	(0.2:tr)	(0.6:tr)	(4:0.5)	(6:0.8)	(15:2)	(0.2:tr)	(0.3:tr)	(0.6:tr)
		3563	3538	3563	3593	3636	3713	3713	3774	3816	3892	4017
		(1.7:0.2)	(0.7:0.1)	(1.7:0.2)	(8:1.1)	(7:1.0)	(7:1.0)	(12:1.6)	(5:0.7)	(2:0.3)	(1.1:0.1)	(0.4:tr)
3577		3548	3577	3603	3645	3703	3742	3794	3820	3910	4058	
(0.4:tr)		(0.7:0.1)	(0.4:tr)	(2:0.3)	(4:0.5)	(3:0.4)	(3:0.4)	(7:1.0)	(1.6:0.2)	(0.4:tr)	(0.2:tr)	
3588		3559	3588	3559	3618	3667	3754	3805	3832	3917		
(0.2:tr)		(0.3:tr)	(0.2:tr)	(0.3:tr)	(9:1.2)	(4:0.5)	(100:14)	(4:0.5)	(4:0.5)	(0.2:tr)		
3574		3574	3574	3574	3646	3701	3779	3822	3841	3926		
(7:1.0)		(7:1.0)	(7:1.0)	(7:1.0)	(6:tr)	(6:tr)	(17:2)	(42:6)	(0.3:tr)	(0.5:tr)		
3591		3591	3591	3591	3657	3712	3823	3845	3873	3953		
(1.1:0.1)		(1.1:0.1)	(1.1:0.1)	(1.1:0.1)	(4:0.5)	(58:7.8)	(3:0.4)	(4:0.5)	(0.7:0.1)	(2:0.2)		
3603		3603	3603	3603	3665	3734	3832	3904	3889	3970		
(0.2:tr)		(0.2:tr)	(0.2:tr)	(0.2:tr)	(3:0.4)	(1.9:0.3)	(3:0.4)	(0.8:0.1)	(19:3)	(1.0:0.1)		
3617		3617	3617	3617	3699	3755	3921	3921	3921			

A-4	(0.2:tr)	(15:2)	(5:0.7)	(0.5:tr)	(0.2:tr)		
	3630	3711	3769	3963	3879	3921	4005
	(0.9:0.1)	(6:0.8)	(5:0.7)	(1.4:0.2)	(0.2:tr)	(1.1:0.1)	(0.2:tr)
	3652	3721	3782		3964	3964	4031
	(9:1.2)	(0.9:0.1)	(1.8:0.2)		(7:1.0)	(7:1.0)	(0.6:tr)
	3714	3756	3802		3992	3992	4057
	(1.9:0.3)	(1.0:0.1)	(3:0.4)		(0.2:tr)	(0.2:tr)	(0.3:tr)
		3870			4018	4018	4082
		(0.3:tr)			(0.4:tr)	(0.4:tr)	(0.1:tr)
A-6							
A-8							

* 1st relative to C₅₂A-2 (KRI = 3754) = 100%; 2nd relative to total petroporphyrins = 100%.

work, to allow future expansion of this type of figure to further samples. In addition, $A(n)$, $A-2(n)$, $A-4(n)$, $A-6(n)$ and $A-8(n)$ appear; these "series" contain the unidentified components which can not be assigned to any of the series co-chromatographed to date.

Boscan crude oil

Fig. 1c shows the RIC (m/z 545-850) obtained from the total petroporphyrins of Boscan oil analysed as their $(\text{TBDMSO})_2\text{Si}$ derivatives, and displayed over the KRI range 3400-4300; some 30 peaks are fully or partially resolved. Considerable co-elution of components is occurring, as evidenced later by mass chromatography. The m/z range of 545-850 shows the "total porphyrin chromatogram", and does not display the co-injected n -alkane retention index standards. Single-ion mass chromatograms were examined for the intense $(M-131)^+$ ions of all alkyl porphyrins from C_{20} to C_{42} , and for the classes A, A-2, A-4, A-6 and A-8. The porphyrins present were of the carbon numbers and classes listed in Table IV. "Genuine" components were assigned after checking of mass spectra as for La Luna. Quantification of the detected porphyrin derivatives was performed by the usual method and is therefore subject to the same errors arising when two porphyrins, with masses differing by two a.m.u., co-elute. Such instances of co-elution occurred 43 times in the analysis of Boscan oil. As before, therefore, the approximate quantification adopted was simply to use the peak areas of the characteristic $(M-131)^+$ ions in the GC-MS data. These areas were obtained from RI lists, output by program RRI. Table IV contains details of each porphyrin detected in GC-MS analysis of the petroporphyrins of Boscan oil (224 in all), its class, carbon number, KRI, and abundance (relative to the C_{32} A-2 porphyrin of KRI = 3754, structure 2a, and also as a percentage fraction of the total petroporphyrins).

To allow further investigation of the tabulated petroporphyrins, Kováts' plots were prepared as before. The five plots produced appear in Fig. 3b, where comparative co-plotting with La Luna has been performed after applying the same threshold values. As was done for Fig. 3a, proposed pseudo-homologous series are marked by dashed lines such that the components of these series are structurally related to co-injected standards. The same five series were identified as were found in Gilsonite bitumen and La Luna shale.

Histograms were prepared for these series, showing each component with its KRI value and relative abundance. In each case the abundances are presented as percent fractions of the abundance of the C_{32} A-2 of KRI = 3754 (structure 2a). The histograms appear in Fig. 5c, forming distribution profiles for these five pseudo-homologous series. Histograms of abundance vs. carbon number for each class (A, A-2, A-4, A-6, A-8) of porphyrins present in Boscan oil are presented in Fig. 6c, for comparison with Gilsonite (Fig. 6a), and La Luna shale (Fig. 6b). Fig. 7c contains similar histograms, plotted for all 7 series for which standards were available for co-injection, though two of these, A-2(3) and A-2(4), were not present in any of the three samples studied to date (see Table I).

Fully alkylated Boscan porphyrins

After acetylation and removal of β -unsubstituted porphyrins, the fully alkylated porphyrins of Boscan oil were derivatised and GC-MS analysis performed as

for the total petroporphyrin mixture. The resultant GC-MS data were processed by the methods set out previously. Co-injections were not performed, since the identities of the standard compounds are readily obtained by comparison of the retention and mass spectral characteristics (especially Fig. 4) with those for the total mixtures (especially Fig. 3b).

Fig. 2b is the RIC, where it is compared with that for the fully alkylated fraction of petroporphyrins from Gilsonite (Fig. 2a). Comparison of Fig. 2a with Fig. 1a and Fig. 2b with Fig. 1c, reveals that the distribution of components is greatly simplified by removal of the β -unsubstituted components. The mass chromatograms obtained for the fully alkylated petroporphyrins of Boscan oil were cross-checked with the mass spectra, quantified and used to prepare a table similar to Table IV. Comparison with the total mixture (Table IV) revealed a reduction in the number of petroporphyrins detected after acetylation and removal of β -unsubstituted compounds from 224 to 87. This simplification is apparent in the Kováts' plots for the fully alkylated fraction, Fig. 4, when compared with the equivalent plots from the total petroporphyrins, Fig. 3b. Fig. 4 compares the fully alkylated porphyrin fractions of Gilsonite bitumen and Boscan oil in the same way as Fig. 3 compared the total porphyrin distributions of Gilsonite and La Luna (Fig. 3a), and La Luna and Boscan (Fig. 3b).

DISCUSSION

Origin of samples

The two samples analysed in this work were obtained from the Maracaibo Basin area of northwestern Venezuela. This basin formed during the Oligocene epoch, and has been described⁴⁵.

Sedimentation of the area now occupied by the basin began in the early Cretaceous with the transgression of a marine environment from the north, which by the end of the Early Cretaceous had covered the major part of the basin. In this marine environment were laid down the rocks of the La Luna formation. This is a thinly-bedded to finely-laminated, organically-rich, shaley limestone of Cretaceous age (*ca.* 90 million years¹⁵). It is widespread throughout northern South America, where similar sediments have been detected in eastern Venezuela, Trinidad, Colombia and Ecuador¹⁵.

The deposition of the La Luna formation is believed to have occurred in an anoxic marine environment, as a result of the existence of a stratified water column. The high sulphur content, up to 10% of the organic extract, of the La Luna formation suggests that active sulphate reduction was occurring at this time⁴⁶.

The La Luna formation has been proposed^{15,16} to be the source rock of the oils of the various reservoirs of northwestern Venezuela. A study based on the petroporphyrin content of crude oils and sediments of the Basin established a direct genetic relationship between the La Luna formation and a range of crude oils from the Maracaibo Basin, including certain Boscan oils¹⁷.

The La Luna shale sample used in the present study is taken from an exposure of the formation in the La Luna type area on the western border of the Maracaibo Basin. It was supplied by Dr. F. Cassani (INTEVEP, Venezuela), and no precise information of its maximum depth of burial and/or temperature is available.

TABLE IV
 PETROPORPHYRINS DETECTED BY GC-MS ANALYSIS OF BOSCAN OIL
 tr = less than 0.1% of total petroporphyrins.

Class	Carbon number, retention index (KRI), relative abundance (%) [*]	27	28	29	30	31	32	33	34	35	36	37	38	
A	3442	3455	3493	3539	3580	3622	3664	3721	3785	3857	4023	4052		
	(1.1:0.1)	(0.3:tr)	(8:1.0)	(25:3)	(40:5)	(14:1.7)	(0.3:tr)	(2:0.2)	(0.3:tr)	(0.1:tr)	(0.3:tr)	(0.2:tr)		
	3447	3482	3528	3572	3603	3647	3684	3732	3798	3887	4031	4075		
	(0.5:tr)	(13:1.6)	(19:2)	(6:0.7)	(10:1.2)	(20:2)	(13:1.6)	(2:0.2)	(0.4:tr)	(0.6:tr)	(0.1:tr)	(0.1:tr)		
	3470	3492	3537	3580	3626	3673	3715	3756	3821	3899	4047	4116		
	(0.7:tr)	(9:1.1)	(24:3)	(31:4)	(1:0:0.1)	(6:0.7)	(14:1.7)	(10:1.2)	(3:0.4)	(0.7:tr)	(0.2:tr)	(0.2:tr)		
	3481	3525	3551	3593	3633	3697	3756	3779	3840	3927	4072			
	(0.5:tr)	(9:1.1)	(2:0.2)	(3:0.4)	(7:0.8)	(2:0.2)	(6:0.7)	(3:0.4)	(2:0.2)	(0.7:tr)	(0.1:tr)			
		3536	3580	3607	3649	3717	3762	3802	3855	3945	4076			
		(0.9:0.1)	(3:0.4)	(4:0.5)	(5:0.6)	(12:1.4)	(3:0.4)	(3:0.4)	(0.4:tr)	(0.4:tr)	(0.1:tr)			
		3545	3593	3620	3670	3778	3790	3832	3889	3978				
		(0.7:tr)	(3:04)	(3:0.4)	(3:0.4)	(0.8:0.1)	(0.9:0.1)	(3:0.4)	(3:0.4)	(0.6:tr)				
						(1.5:0.2)	(1:0:0.1)							
						3806								
					(2:0.2)									
A-2	3538	3534	3576	3607	3655	3756	3801	3889	3893	4030	4105			
	(1.0:0.1)	(1.0:0.1)	(0.8:0.1)	(0.4:tr)	(1.4:0.2)	(13:1.6)	(0.5:tr)	(2:0.2)	(0.3:tr)	(0.3:tr)	(0.2:tr)			
	3546	3576	3591	3634	3714	3776	3817	3923	3925	4057				
	(0.1:tr)	(3:0.4)	(0.9:0.1)	(1.6:0.2)	(11:1.3)	(3:0.4)	(1.6:0.2)	(0.5:tr)	(0.2:tr)	(0.3:tr)				
	3563	3581	3620	3666	3756	3791	3833	3954	3946	4115				
	(0.5:tr)	(3:0.4)	(10:1.2)	(3:0.4)	(100:12)	(6:0.7)	(4:0.5)	(2:0.2)	(0.2:tr)	(0.2:tr)				
	3583	3622	3661	3715	3782	3807	3849	3972	3960	4148				
	(0.3:tr)	(0.3:tr)	(23:3)	(80:10)	(21:3)	(4:0.5)	(1.6:0.2)	(3:0.4)	(0.3:tr)	(0.1:tr)				
	3606	3650	3696	3733	3822	3823	3861	4001	3965					
	(0.2:tr)	(4:0.5)	(6:0.7)	(0.1:tr)	(0.6:tr)	(28:3)	(0.2:tr)	(0.5:tr)	(0.4:tr)					

TABLE IV (continued)

Class	27	28	29	30	31	32	33	34	35	36	37	38
	Carbon number, retention index (KRI), relative abundance (%)*											
A-8					3974 (0.7:tr)	3988 (0.3:tr)	4071 (0.5:tr)	4104 (0.1:tr)	4171 (0.1:tr)	4232 (0.2:tr)		
					3987 (0.1:tr)	4030 (0.3:tr)	4110 (7:0.8)	4110 (0.7:tr)	4186 (0.3:tr)	4244 (0.2:tr)		
						4066 (0.4:tr)	4119 (0.2:tr)	4144 (0.4:tr)	4203 (0.2:tr)	4250 (0.1:tr)		
						4074 (1.5:0.2)		4158 (0.2:tr)	4216 (0.2:tr)	4262 (0.2:tr)		
						4106 (0.2:tr)		4172 (0.3:tr)	4228 (0.2:tr)	4277 (0.2:tr)		
								4179 (0.1:tr)				

* 1st relative to C₃₂A-2 (KRI = 3756) = 100%; 2nd relative to total petroporphyrins = 100%.

The Boscan oil field is situated in the northwestern part of the Maracaibo Basin, west of the Maracaibo Lake and east of the La Luna shale outcrop areas. This field has been described in detail²⁹. The oil-bearing sandstones (Upper Eocene, *ca.* 40 m years) can be detected over a large depth range, from *ca.* 1500 m in the north to over 3000 m in the south. As a result of these differences in depth, the temperatures of the oils in the reservoir also vary, between *ca.* 65°C and 85°C¹⁹. The Boscan oil sample examined in the present paper was obtained from well 8E-4 at a depth of *ca.* 2230–2310 m, with a formation temperature estimated from present-day geothermal gradient⁴⁷ as 77°C. These two oil-source samples are compared and contrasted herein, by GC-MS examination of their petroporphyrins, with the unrelated bitumen Gilsonite.

Gilsonite bitumen is found in veins in the sandstone Uinta formation of Utah (U.S.A.), and is believed to be sourced from the Parachute Creek member of the underlying Green River formation^{48,49}. The shales of the Green River formation were deposited by Lake Uinta during the Eocene. During most of its existence, this lake was stratified, with an aerated upper layer containing abundant life, and a saline, anoxic, lower layer. The salinity (sulphates, carbonates, bicarbonates, only small amounts of chlorides) increased through the life-span of the lake so that the Gilsonite source beds were laid down in a strongly saline anoxic non-marine environment^{50–53}. It is estimated from the present-day geothermal gradient, that the Gilsonite source beds, 1400 m deep, have experienced temperatures no higher than 50°C.

Thus, Gilsonite, studied in our earlier publication¹⁴, is of immature, non-marine origin, contrasting with the more mature, marine La Luna shale and the further matured Boscan oil, sourced from the La Luna shale.

Petroporphyrin analyses

As earlier reported for Gilsonite¹⁴, in Boscan oil and La Luna shale five pseudo-homologous series of petroporphyrins have been partially identified. Certain members of these series co-chromatograph with (or have near-identical KRI values to) known porphyrin derivatives and so are presumed to have structures identical to, or isomeric with, those standards. The other members of the series may therefore be assumed to have closely related structures of different carbon number. From arguments presented previously¹⁴, these series, containing 32 compounds in both Boscan oil and in La Luna shale, and representing over 80% of the total porphyrin content of each, are suggested to possess *n*-alkyl substituents only.

Two of the series, A(2) and A(3), are each known to contain a C₂₉ member with two ethyl and five methyl substituents, and therefore one unsubstituted β -position. The two series are therefore each proposed to consist of monounsubstituted aetioporphyryns. A(2) and A(3) are separated by *ca.* 10 KRI units, with the members of A(2) eluting earlier. This KRI difference is presumably an effect of the relationship of the free β -H to the other groups, this relation being somehow different in the two series. Clearly, it would be very useful to possess complete and unambiguous structural assignments of these two C₂₉ isomers.

Full structural determination has not been carried out for most of these compounds. Hence, the assumption that points lying on straight lines on the plots represent porphyrins of related structures is not fully tested. However, all those instances in which known structures have been co-injected support this proposition. Com-

pounds of related type (*e.g.* the fully-alkylated aetios) fall on one such line, compounds of different types (*e.g.* 13¹-methyl-13,15-ethanoporphyrins and 13,15-ethanoporphyrins) fall on different lines. Two other A-2 types, a 15¹-methyl-15,17-propanoporphyrin and two 15,17-butanoporphyrins, which are not present in these samples, fall at much larger KRI values and, presumably, would lie on other straight lines in samples known to contain series of these types (*e.g.* Serpiano oil shale^{32,37}).

Petroporphyrin distributions

Histograms were prepared for these five series of petroporphyrins. As revealed by GC-MS analysis of La Luna shale, they have carbon number ranges and maxima as set out in Fig. 5b. In general, the abundances of the compounds show an increase from low carbon numbers, up to a maximum, and then decrease again at high carbon numbers. A slight deviation occurs in series A-2(1), a series of 13¹-methyl-13,15-ethanoporphyrins, where the C₃₁ member is lower in abundance than its C₃₀ and C₃₂ counterparts, producing an apparently "bimodal," distribution. This "bimodality" is more evident in series A(3), which has maxima at C₃₀ and C₃₃. In Boscan oil, the distribution profiles of the five series are very similar to the corresponding La Luna series. Their carbon number ranges and maxima are presented in Fig. 5c. Minor differences from La Luna are apparent:

(i) In series A(3), mono β -unsubstituted aetioporphyrins, a C₃₅ component was detected in Boscan oil, but not in La Luna shale.

(ii) In series A-2(1), a fully alkylated series of 13¹-methyl-13,15-ethanoporphyrins, a C₂₈ member was found in the shale, but was absent from Boscan oil.

(iii) In series A-2(2), the major series of fully alkylated 13,15-ethanoporphyrins, the C₃₀ and C₃₁ components are relatively much more abundant in Boscan oil than in La Luna shale.

Fig. 5 (the distribution histogram for Gilsonite, Boscan and La Luna) allows simple visual comparison of the major components of each sample. The porphyrin distribution of Boscan crude oil is similar to that of its source rock, emphasising the potential utility of GC-MS analysis in the correlation of geochemical materials by their petroporphyrin distributions. In contrast the petroporphyrins of Gilsonite¹⁴ show a different distribution to those of the two Maracaibo Basin samples:

(i) Though their carbon number ranges are similar, the five partially identified series, A(1), A(2), A(3), A-2(1) and A-2(2), all maximise one carbon number lower in Gilsonite.

(ii) The Boscan and La Luna samples each contain more porphyrins, particularly the later-eluting components and the components with higher degrees of unsaturation. Thus, in the Maracaibo Basin samples, there are more aetioporphyrins with KRI values higher than those of series A(3), more A-2 porphyrins with KRI values above those of series A-2(2) and more porphyrins of classes A-4 and A-6, while the A-8 class is absent from Gilsonite. One possibility is that these high carbon number homologues represent the remains of bacteriochlorophyll precursors⁵⁴.

Acetylation of petroporphyrins

The Friedel-Crafts acetylation procedure, as applied to petroporphyrins⁴⁰, is expected to replace any aromatic hydrogen atom by an acetyl function. The acetylated species may then be separated from the remaining porphyrins by TLC. How-

ever, it should be noted that in the supposed fully alkylated fraction of Boscan petroporphyrins, compounds of classes A-6 and A-8 remain, though at much reduced relative abundance. Since porphyrins of these classes are known^{6,18} to possess a fused benzo-ring structure (*e.g.* 4 and 5), they should be acetylated and removed; it may be that the conditions employed for the reaction were not sufficiently forcing to acetylate fully compounds of this type. In particular, longer reaction times may be required. Similar observations have been made in the case of Gilsonite¹⁴, where certain A-6 class porphyrins remain after acetylation, and where the higher carbon number members of series A(3) were not removed, despite the fact that the C₂₉ member (1c), at least, possesses an unsubstituted β -position.

Comparative C-GC-MS analyses of petroporphyrin distributions

The use of C-GC-MS analysis with comparison of graphical displays shows differences and similarities among and between the porphyrin distributions of different samples. Thus, Figs. 5 and 6 show strong similarities between the related La Luna shale and Boscan oil, with significant differences from the Gilsonite bitumen.

By comparison of Fig. 5 (which shows abundances for all identified components and their pseudo-homologues) with Fig. 6 (containing abundance data for the sum of all porphyrins present), it is possible to determine easily the presence of significant components of unknown structure. Tables III and IV then give the KRI values of the relevant compounds. These data are useful to the planning of future structural elucidation studies. As more structures are completely assigned to the porphyrins, it will become possible to unravel the geochemical processes operating to produce, and alter, the distributions observed in the GC-MS analyses. Knowledge of the chemical processes may, in turn, enable specific features of the porphyrin distributions to be employed as indicators of palaeoenvironment of the original site of deposition of the sedimentary organic matter and/or the thermal maturity reached by such organic matter.

Detailed numerical correlation will require the use of statistical software packages and some means of entering GC-MS data, either "raw" or partially processed. One approach is the use of a "reverse search" procedure¹³. Statistical treatment of C-GC-MS data will provide opportunities for the numerical investigation of maturity and palaeoenvironmental parameters.

CONCLUSIONS

GC-MS analysis of the petroporphyrins of Boscan oil and its source rock, La Luna shale, has revealed the presence of large numbers of individual porphyrins. Plotting the KRI values of the (TBDMSO)₂Si derivatives against the carbon numbers of the parent porphyrins produces a number of straight-line relationships between the points. These are proposed to be pseudo-homologous series of structurally related porphyrins. Co-injection experiments with compounds of known, or partially known, structures provide some information regarding the nature of these series. Comparison of the distributions of porphyrins within these series, their carbon numbers and relative abundances, demonstrates the similarity of these two related samples, at least in regard to their major components. These two Maracaibo Basin samples are demonstrably different in their porphyrin distributions from the unrelated Gilsonite bitumen.

The following conclusions may be drawn:

(i) GC-MS analysis of petroporphyrin fractions, as (TBDMSO)₂Si derivatives, yields useful and detailed information on their alkyl porphyrin content. The class, carbon number and abundance are obtained directly, and co-injection and acetylation experiments provide some information on the structures of these porphyrins.

(ii) Visual comparisons of relative abundance profiles produced for five major pseudo-homologous series demonstrate the high degree of similarity between a crude oil (Boscan) and its source rock (La Luna).

(iii) The ratio of A-2 class to A class porphyrins (generally termed the DPEP-aetio ratio), which has been suggested, and employed, as a maturity measure of geological materials³, is readily obtained from GC-MS data.

(iv) The procedure described reveals petroporphyrin distributions of geological or similar samples and, hence, provides information complementary to that gained from other biomarkers, which may include oil to source correlation, assessment of maturity and palaeoenvironment of deposition, evidence for migration and effects (if any) of biodegradation.

ACKNOWLEDGEMENTS

The authors thank Mr. C. L. Saunders, Mrs. A. P. Gowar and Ms. L. Dyas for assistance with GC-MS and computer facilities. Professor P. S. Clezy and Dr. J. G. Erdman are thanked for gifts of free-base octamethylporphyrin and aetioporphyrin standards, as are Drs. M. I. Chicarelli, G. A. Wolff and J. R. Maxwell for characterised free-base porphyrins isolated from geological samples. Dr. F. Cassani (INTEVEP, Venezuela) is thanked for the La Luna shale and the late Dr. W. Seifert (Chevron, U.S.A.) for the Boscan 8E-4 oil sample. The Science and Engineering Research Council is thanked for financial support (GR/B/04471) and a Research Studentship (J.P.G.), as is the British Petroleum plc for an EMRA award (R.P.E.) and the National Aeronautics and Space Administration (sub-contract from NGL 05-003-003, the University of California, San Francisco). The Natural Environment Research Council's grants (GR3/2951 and GR3/3758) provided GC-MS and MS computing facilities.

REFERENCES

- 1 A. S. MacKenzie, J. M. E. Quirke and J. R. Maxwell, in A. G. Douglas and J. R. Maxwell (Editors), *Advances in Organic Geochemistry 1979*, Pergamon Press, Oxford, 1980, pp. 239-248.
- 2 E. W. Baker and J. W. Louda, in M. Bjorøy, P. Albrecht, C. Cornford, K. de Groot, G. Eglinton, E. Galimov, D. Leythausen, R. Pelet, J. Rullkötter and G. Speers (Editors), *Advances in Organic Geochemistry 1981*, Heyden and Sons, London, 1983, pp. 401-421.
- 3 A. J. G. Barwise and P. J. D. Park, in M. Bjorøy, P. Albrecht, C. Cornford, K. de Groot, G. Eglinton, E. Galimov, D. Leythausen, R. Pelet, J. Rullkötter and G. Speers (Editors), *Advances in Organic Geochemistry 1981*, Heyden and Sons, London, 1983, pp. 668-674.
- 4 A. J. G. Barwise and I. Roberts, *Org. Geochem.*, 6 (1984) 167-176.
- 5 E. W. Baker, *J. Am. Chem. Soc.*, 88 (1966) 2311-2315.
- 6 E. W. Baker, T. F. Yen, J. P. Dickie, R. E. Rhodes and L. F. Clarke, *J. Am. Chem. Soc.*, 89 (1967) 3631-3639.
- 7 S. K. Hajlbrahim, P. J. C. Tibbetts, C. D. Watts, J. R. Maxwell, G. Eglinton, H. Colin and G. Guiochon, *Anal. Chem.*, 50 (1978) 549-553.

- 8 G. Eglinton, S. K. Hajlbrahim, J. R. Maxwell and J. M. E. Quirke, in A. G. Douglas and J. R. Maxwell (Editors), *Advances in Organic Geochemistry 1979*, Pergamon Press, Oxford, 1980, pp. 193–203.
- 9 P. J. Marriott, J. P. Gill, R. P. Evershed, C. S. Hein and G. Eglinton, *J. Chromatogr.*, 301 (1984) 107–128.
- 10 G. Eglinton, R. P. Evershed and J. P. Gill, *Org. Geochem.*, 6 (1984) 157–165.
- 11 P. J. Marriott, J. P. Gill and G. Eglinton, *J. Chromatogr.*, 249 (1982) 291–310.
- 12 P. J. Marriott, J. P. Gill, R. P. Evershed, G. Eglinton and J. R. Maxwell, *Chromatographia*, 16 (1982) 304–308.
- 13 C. S. Hein, J. P. Gill, R. P. Evershed and G. Eglinton, *Anal. Chem.*, 57 (1985) 1872–1879.
- 14 J. P. Gill, R. P. Evershed, M. I. Chicarelli, G. A. Wolff, J. R. Maxwell and G. Eglinton, *J. Chromatogr.*, 350 (1985) 37–62.
- 15 H. D. Hedburg, *Bull. Am. Assoc. Petrol. Geol.*, 48 (1964) 1755–1803.
- 16 S. Talukdar, O. Gallango and M. Chin-A-Lien, *Org. Geochem.*, in press.
- 17 J. A. Gransch and E. Eisma, in G. D. Hobson and G. C. Speers (Editors), *Advances in Organic Geochemistry 1966*, Pergamon Press, Oxford, 1970, pp. 193–203.
- 18 S. Kaur, M. I. Chicarelli and J. R. Maxwell, *J. Am. Chem. Soc.*, 108 (1986) 1347–1348.
- 19 B. M. Didyk, *Ph.D. Thesis*, University of Bristol, Bristol, 1975.
- 20 A. J. G. Barwise and E. V. Whitehead, in A. G. Douglas and J. R. Maxwell (Editors), *Advances in Organic Geochemistry 1979*, Pergamon Press, Oxford, 1980, pp. 181–192.
- 21 T. F. Yen, L. J. Boucher, J. P. Dickie, E. C. Tynan and G. B. Vaughan, *J. Inst. Pet.*, 55 (1969) 87–99.
- 22 G. W. Hodgson, M. Strosher and D. J. Casagrande, in H. R. von Gaertner and H. Wehner (Editors), *Advances in Organic Geochemistry 1971*, Pergamon Press, Oxford, 1972, pp. 151–161.
- 23 E. W. Baker and S. E. Palmer, in D. Dolphin (Editor), *The Porphyrins*, Vol. I, Academic Press, New York, 1978, pp. 486–552.
- 24 J. M. E. Quirke, G. J. Shaw, P. D. Soper and J. R. Maxwell, *Tetrahedron*, 36 (1980) 3261–3267.
- 25 Y. I. A. Alturki, *Ph.D. Thesis*, University of Bristol, Bristol, 1972.
- 26 S. K. Hajlbrahim, J. M. E. Quirke and G. Eglinton, *Chem. Geol.*, 32 (1981) 173–188.
- 27 D. B. Boylan, Y. I. A. Alturki and G. Eglinton, in P. A. Schenck and I. Havenaar (Editors), *Advances in Organic Geochemistry 1968*, Pergamon Press, Oxford, 1969, pp. 227–240.
- 28 R. Alexander, G. Eglinton, J. P. Gill and J. K. Volkman, *J. High Resolut. Chromatogr. Chromatogr. Commun.*, 3 (1980) 521.
- 29 J. A. F. Sutherland, in R. E. King (Editor), *Stratigraphic Oil and Gas Fields: Classification, Exploration Methods and Case Histories*, Am. Assoc. Petrol. Geol. Memoir 16, 1972, pp. 559–567.
- 30 J. G. Erdman, *U.S. Pat.*, 3,190,829 (1965).
- 31 S. K. Hajlbrahim, *Ph.D. Thesis*, University of Bristol, Bristol, 1978.
- 32 M. I. Chicarelli, *Ph.D. Thesis*, University of Bristol, Bristol, 1985.
- 33 J. M. E. Quirke, G. Eglinton and J. R. Maxwell, *J. Am. Chem. Soc.*, 101 (1979) 7693–7697.
- 34 G. A. Wolff, *Ph.D. Thesis*, University of Bristol, Bristol, 1983.
- 35 G. A. Wolff, M. I. Chicarelli, G. J. Shaw, R. P. Evershed, J. M. E. Quirke and J. R. Maxwell, *Tetrahedron*, 40 (1984) 3777–3786.
- 36 M. I. Chicarelli, J. R. Maxwell and R. A. Pitt, in preparation.
- 37 M. I. Chicarelli, G. A. Wolff, M. Murray and J. R. Maxwell, *Tetrahedron*, 40 (1984) 4033–4039.
- 38 G. A. Wolff, M. Murray, J. R. Maxwell, B. K. Hunter and J. K. M. Sanders, *J. Chem. Soc., Chem. Commun.*, (1983) 922–924.
- 39 J.-H. Fuhrhop and K. M. Smith, in K. M. Smith (Editor), *Porphyryns and Metalloporphyryns*, Elsevier, Amsterdam, 1976, p. 798.
- 40 J. M. E. Quirke, in M. Bjorøy, P. Albrecht, C. Cornford, K. de Groot, G. Eglinton, E. Galimov, D. Leythausser, R. Pelet, J. Rullkötter and G. Speers (Editors), *Advances in Organic Geochemistry 1981*, Heyden and Sons, London, 1983, pp. 733–745.
- 41 C. S. Hein and G. Eglinton, in preparation.
- 42 E. Kováts, *Helv. Chim. Acta.*, 41 (1958) 1915–1932.
- 43 M. I. Chicarelli and J. R. Maxwell, *Tetrahedron Lett.*, 25 (1984) 4701–4704.
- 44 R. Ocampo, H. J. Callot, P. Albrecht and J. R. Kintzinger, *Tetrahedron Lett.*, 25 (1984) 2589–2592.
- 45 J. B. Miller, K. L. Edwards, P. P. Wolcott, H. W. Anisgard, R. Martin and H. Anderegg, in *Habitat of Oil Symposium, New York 1955*, Am. Assoc. Petrol. Geol., Tulsa, 1958, pp. 601–640.
- 46 J. A. Gransch and P. Posthuma, in B. Tissot and F. Bienner (Editors), *Advances in Organic Geochemistry 1973*, Editions Technip, Paris, 1974, pp. 727–739.

- 47 E. E. Hagan, personal communication (1974).
- 48 J. M. Hunt, F. Stewart and P. A. Dickey, *Bull. Am. Assoc. Petrol. Geol.*, 38 (1954) 1671-1698.
- 49 K. G. Bell and J. M. Hunt, in I. Breger (Editor), *Organic Geochemistry*, Pergamon Press, London, 1963, pp. 333-366.
- 50 W. H. Bradley, *U.S. Geol. Survey Prof. Paper 496-A*, 1964.
- 51 W. H. Bradley and H. P. Euger, *U.S. Geol. Survey Prof. Paper 496-B*, 1969.
- 52 W. H. Bradley, *Bull. Geol. Soc. Am.*, 81 (1970) 985-1000.
- 53 W. H. Bradley, *Bull. Geol. Soc. Am.*, 84 (1973) 1121-1124.
- 54 R. Ocampo, H. J. Callot and P. Albrecht, *J. Chem. Soc., Chem. Commun.*, (1985) 200-201.